PAPER • OPEN ACCESS

Collective response of microrobotic swarms to external threats

To cite this article: Chun-Jen Chen and Clemens Bechinger 2022 *New J. Phys.* **24** 033001

New Journal of Physics
The open access journal at the forefront of physics

Deutsche Physikalische Gesellschaft DPG
IOP Institute of Physics

Published in partnership with: Deutsche Physikalische Gesellschaft and the Institute of Physics

OPEN ACCESS

RECEIVED
20 August 2021

REVISED
15 January 2022

ACCEPTED FOR PUBLICATION
9 February 2022

PUBLISHED
7 March 2022

PAPER

Collective response of microrobotic swarms to external threats

Chun-Jen Chen[1] and Clemens Bechinger[1,2,*]

[1] Fachbereich Physik, Universität Konstanz, 78464 Konstanz, Germany
[2] Centre for the Advanced Study of Collective Behaviour, Universität Konstanz, 78464 Konstanz, Germany
[*] Author to whom any correspondence should be addressed.

E-mail: clemens.bechinger@uni-konstanz.de

Keywords: collective behaviour, active Brownian colloids, collective decision-making

Supplementary material for this article is available online

Abstract

Many animal species organize within groups to achieve advantages compared to being isolated. Such advantages can be found e.g. in collective responses which are less prone to individual failures or noise and thus provide better group performance. Inspired by social animals, here we demonstrate with a swarm of microrobots made from programmable active colloidal particles (APs) that their escape from a hazardous area can originate from a cooperative group formation. As a consequence, the escape efficiency remains almost unchanged even when half of the APs are not responding to the threat. Our results not only confirm that incomplete or missing individual information in robotic swarms can be compensated by other group members but also suggest strategies to increase the responsiveness and fault-tolerance of robotic swarms when performing tasks in complex environments.

1. Introduction

Many living species arrange themselves into functional cohesive groups. Remarkably, such behavior can be achieved without centralized control but results from so-called interaction rules which determine the actions performed by each member in response to their peers. Even though the specific reason for the formation of collective states is not always obvious, it is generally assumed that they provide collective benefits that exceed the sum of individual abilities within the group [1–4]. There are many examples demonstrating collective states to be more efficient than solitary organisms with respect, e.g. to foraging [5], vigilance [6–8], heat preservation [9] or transport of heavy loads [10, 11]. Knowledge regarding these interaction rules and their performance is not only important in the study of living systems but also enables progress and innovation in other areas of science [12–14]. For example, the optimization of group performance, both in efficiency and reliability, is one key issue in the context of swarms formed by microscopic robotic systems [15, 16] which are substantial regarding their envisaged potential applications such as drug delivery and active assembly processes.

As a specific example for a collective benefit, here we experimentally investigate the collective escape motion of a cohesive swarm of active particles (APs) from a static hazardous area. This situation is motivated by the behavior of animal groups, e.g. fish schools which are known to move away from high temperature regions [17], and avoid shallow areas [18]. Another example is the response of animal groups to the early discovery of a predator which is still far away. Certain animal groups respond to risks collectively e.g. by the formation of rotational states, i.e. swirls [19], which suggests potential benefits against predation in numerical simulations [20–22]. In addition, when the group remains compact during the escape motion, this enables more variety and complexity regarding their defense compared to being scattered [3, 8, 23–25]. Similar to living systems, enhanced perception and responsiveness and the ability of complex tasking at the group level is crucial for microrobotic swarms with limited internal complexity. So far, however, it is not clear how interaction rules between individuals must be tailored to allow for synergistic benefits at the group level [26]. For example, when the escape of animals from a predator is

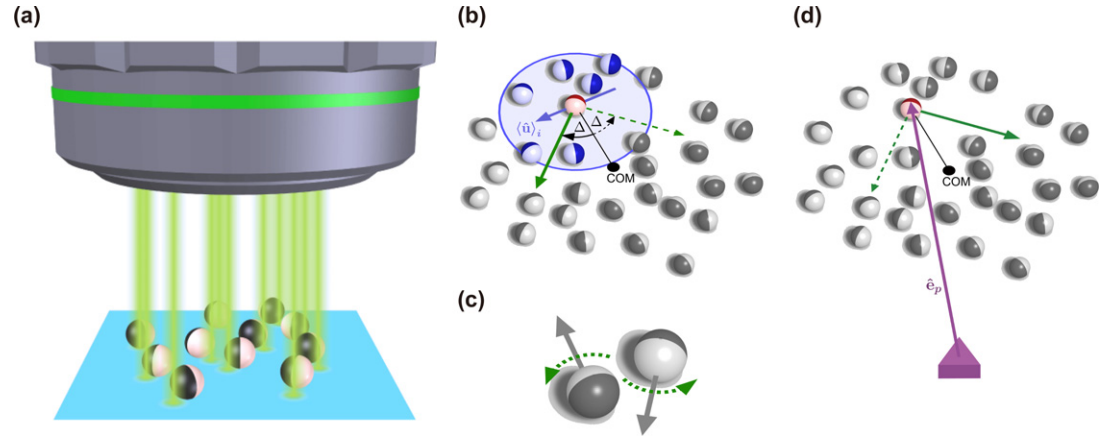

Figure 1. Programmable APs responding to a static threat. (a) Schematic of laser experiment. Each AP is steered by a laser beam that imposes the steering signal determined by the interaction rules shown in (b)–(d). (b) In absence of a threat each AP (one highlighted in red) aims to steer in a direction deviating from the COM by the angle Δ to the left or right (green arrows). The left/right steering decision depends on what direction is closer to the mean orientation of neighbors $\hat{\boldsymbol{u}}_i$ within distance $R_o \approx 4\sigma$ (blue line). In the configuration shown here, the AP follows the solid green arrow. (c) To minimize collisions, APs turn away from each other when their surface-to-surface distance falls below 0.25σ. (d) In presence of a threat, only the left/right steering decision is changed. It becomes independent of $\hat{\boldsymbol{u}}_i$ but only depends on what direction yields the larger alignment with the vector pointing from the threat (purple triangle) to the corresponding AP (purple arrow). In the shown example, the particle follows the solid green arrow.

modeled by a repulsive interaction between individuals and the threat, this easily leads to group splitting which can be detrimental in view of the groups defending performance. Furthermore, a repulsive response to the predator from each individual requires all responding group members to receive and process precise positional information regarding the threat.

Here we demonstrate that an efficient avoidance of a hazardous spot (threat) to a cohesive group of microrobotic APs can be achieved without imposing a repulsion of APs from the threat. In the following we study the response of a rotating group (swirl) since such states are considered as an effective alert strategy of certain animal groups when exposed to higher risk [19, 27]. Swirl formation is also supported by simulations suggesting potential benefits against predation [20–22]. Here As a clear evidence of a collective benefit, we find that the evasive group's motion is only little affected when up to half of the APs are blind to the threat but only respond to their neighbors. This demonstrates that partial or even missing sensory input regarding environmental conditions can be easily compensated in robotic swarms by suitable interaction rules between the group members which allows for genuine team work. Apart from optimizing the efficiency in performing tasks with a given number of robots, this mechanism also increases the robustness of collectives against individual errors regarding their sensorial and motional capabilities.

2. Experimental details

Sensing and communication in microrobotic swarms is achieved using a feed-back loop where the corresponding information and steering signals, determined by social interaction rules, are instantaneously computed externally and then inserted into the system. This type of approach is particularly useful for the control of micron-sized robots with limited autonomous sensing and steering functionalities [28–30] and has also been successfully applied to macroscopic robotic systems [13, 31]. In our work, groups of responsive APs are made from transparent silica particles with diameter $\sigma = 6.3\ \mu$m which are coated on one side with a 80 nm light absorbing carbon cap (methods). They are suspended in a water-lutidine mixture contained in a thin sample cell whose temperature is kept constant and below the fluid's lower demixing temperature $T_c = 34\ ^\circ$C. When an AP is illuminated with a focused laser beam, its cap heats up and induces a local demixing which leads to a fluid flow around the AP [32]. This leads to a two-dimensional (2D) self-propulsive, i.e. active, particle motion, with velocity $\boldsymbol{u} = v\hat{\boldsymbol{u}}$. Here, v corresponds to the magnitude and $\hat{\boldsymbol{u}}$ to the direction of velocity which is opposite to the carbon cap. To make APs behave as microrobots which adjust their motion according to specific social interaction rules, their velocity (magnitude and direction) is controlled individually (as shown in figure 1(a)). This is achieved by scanning the illuminating laser beam rapidly across all APs and by independently adjusting the intensity and laser focus position relative to each cap center [28] (methods). Via feedback-control, this allows APs to stop, move forward or turn to the left and right depending on the chosen interaction rule. Despite certain

similarities with a numerical simulation, it should be realized that in experiments, the APs interact with a true physical environment which leads to additional, e.g. steric, hydrodynamic and phoretic, interactions which are frequently neglected simulation works.

In our experiments, we investigated the response of a cohesive rotating group (swirl) of APs which respond to a suddenly appearing threat. This has been achieved by implementation of social rules similar to milling schools of fish [22, 33]: in absence of a threat, each AP turns in the direction of the group's center of mass (COM). To yield a rotating motion of the group, however, APs move not directly towards the COM but with an angular deviation Δ to the left (+) or the right (−). If not stated otherwise, all experiments were carried out with $\Delta = 56.25°$. The left/right decision is made depending on what direction achieves larger alignment with its neighbors within distance $R_o = 25\ \mu\text{m} \approx 4\sigma$ (figure 1(b)). To minimize particle collisions, they turn away from each other when their clearance is below 0.25σ (figure 1(c)). Application of such rules leads to cohesive swirls which display occasional changes in their sense of rotation due to thermal noise. To model the response of APs to a localized threat, only the individual's preference for swimming to the left or right relative to the COM is modified. Regardless of the next neighbor alignment, in presence of a threat each AP selects that sign of Δ which is pointing farther away from the threat (figure 1(d)). It should be realized that this response corresponds to a mere threat avoidance (in contrast to a threat repulsion) strategy and does not force APs to move opposite to the threat. In fact, even an AP motion towards the threat is possible within this response rule as exemplarily shown by the marked particle in figure 1(d). If not stated otherwise, experiments were performed with $N = 85$ APs but no qualitative differences are observed in the range $N = 65$–165.

3. Experimental results

3.1. Collective response to a stationary threat

Figure 2(a) shows a time series of snapshots with intervals of 200 s each of a swirling group of APs when responding to a static threat. After the threat appears at $t > 0$ s the circular swirl undergoes a sudden reorganization and turns into an arrowhead shaped group which is moving straight away from the threat. This deformation of the group is also revealed by the AP density distribution shown in figure 2(b). Such behavior is indeed surprising given the fact that no direct escape motion opposite to the threat is imposed in the interaction rule (see figure 1(d)). As will be shown further below, the observed escape motion is the result of a collective process but not directly encoded at an individual scale. The escape motion is quantified by the displacement of the center-of-mass (COM) which (without noticeable delay) increases almost linearly for $t > 0$ corresponding to a velocity $v_{\text{COM}} = 0.08\ \mu\text{m s}^{-1}$ being about 10% of the propulsion speed of an isolated AP (figure 2(c)). To quantify the properties of the escaping group, we have further calculated the group's rotation and polarization using the corresponding order parameters

$$O_{\text{R}} = \frac{1}{N}\sum_{i=1}^{N} (\hat{\boldsymbol{r}}_i \times \hat{\boldsymbol{u}}_i) \cdot \hat{\boldsymbol{e}}_z$$

and

$$O_{\text{P}} = \frac{1}{N}\left|\sum_{i=1}^{N} \hat{\boldsymbol{u}}_i\right|,$$

respectively. Here, N is the number of APs, $\hat{\boldsymbol{r}}_i$ the unit vector from the group center to the ith particle, and $\hat{\boldsymbol{e}}_z$ the unit vector perpendicular to the 2D plane of motion. For $t > 0$, O_{R} drops from its initial value to almost zero while O_{P} increases by almost a factor 3 which suggests a transition from a swirl to a flock-like behavior (figure 2(d)). Notably, O_{R} and O_{P} react to the threat without noticeable time-delay.

To understand the collective reorganization of APs when responding to the threat, we evaluated the local vorticity $c(\boldsymbol{r})$ which measures the local degree of circular particle motion within the COM's comoving reference frame (methods). Figure 3 shows $c(\boldsymbol{r})$ together with the particle orientations for different times after the threat appeared. At $t = 0$, $c(\boldsymbol{r})$ is essentially negative (the small positive values at the edge of the group are caused by its finite size) which corresponds to a clockwise rotating group with the vortex center near the COM (figure 3(a)). After the threat appeared, the group responds by forming a second vortex with inverted rotational direction. Importantly, the vortices are symmetrically arranged to the left and right to the axis connecting the threat and the COM (figure 3(c)). This is due to the fact that the swimming direction of each AP (according to the above defined interaction rule) depends on its relative positions to the COM and the threat, respectively. This symmetry axis naturally coincides with the escape direction of the COM and thus explains the collective escape response with a cooperative group formation. From the AP orientations (lower part of figure 3), even though only a small number of APs move in the direction

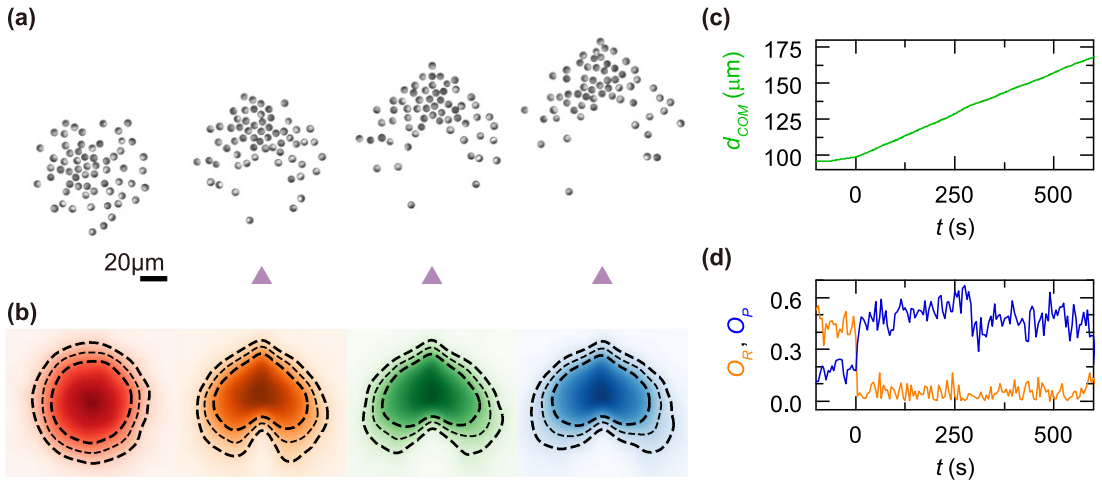

Figure 2. Response of a rotating group of APs to a static threat. (a) Sequence of video images of a swirl formed by $N = 62$ APs with $\Delta = 56.25^\circ$ which is responding to a threat which appears $t > 0$. The time interval between images is 200 s each. (b) Temporal change of the density distribution of an escaping group. Geometrical shape of the escaping flock as a function of time, shown at $t = [0, 200, 400, 600]$ s averaged over 75 groups composed of $N = 85$ with $\Delta = 56.25^\circ$. After the predator appeared, the symmetry of the particle density of APs within the group varies as a function of time until reaches a non-equilibrium steady state after about 300 s. Dashed lines correspond to the contours where the density has reached [52%, 67%, 75%] of the normalized AP density. (c) Temporal change of the COM-threat distance d_{com}. (d) Temporal behavior of the rotation and polarization order parameters O_{R} and O_{P}, respectively.

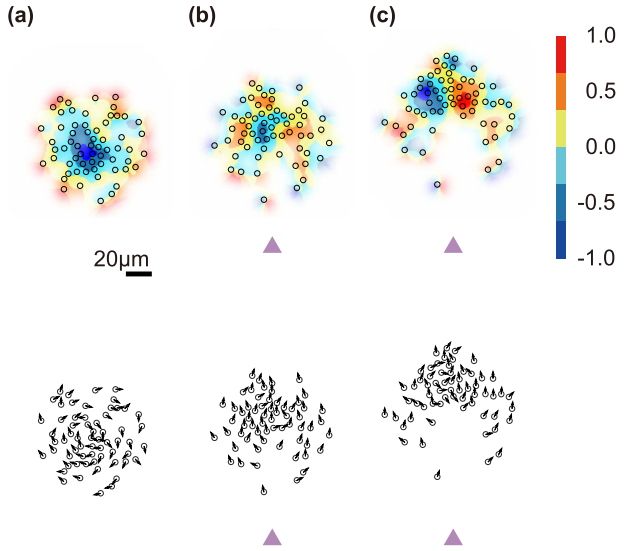

Figure 3. Spatially resolved vorticity and velocity of APs during escape from a stationary threat. (a)–(c) Upper part: color maps of the spatially resolved AP vorticity motion within the COM's comoving frame of reference for times $t = [0, 100, 300]$ s after the threat appeared. Lower part: corresponding particle velocity directions indicated by arrows. The scale bar corresponds to 20 μm.

opposite to the threat either from themselves or from the COM, the collective motion of the entire group points precisely opposite to the threat. This becomes comprehensible as the escape direction is only determined by the overall structure formed by the collective state.

The collective escape behavior of APs is strongly determined by the deviation angle Δ which can be freely chosen in our experiments. Figures 4(a)–(d) shows how the density distribution of the group changes upon varying Δ between 33.75° and 78.75° after the group has reached a steady state where $|O_{\mathrm{R}}|$ and O_{P} remain almost constant. Opposed to the central densest region which remains rather unchanged, the outer regions of the groups expands with increasing Δ. Such behavior is consistent with the increasing size of unperturbed swirls with increasing Δ [34]. We also observe a Δ-dependence of the group's escape velocity v_{COM} which increases about a factor of two and then levels off towards larger Δ (see inset figure 4(e)). After replotting v_{COM} versus $|O_{\mathrm{R}}|$ of the unperturbed swirl, an almost linear relationship is obtained. In other words, Δ values leading to a more pronounced swirl behavior also promote the group's escape motion. At first glance, this result does not seem to be intuitive, as a swirl appears disadvantageous to achieve high

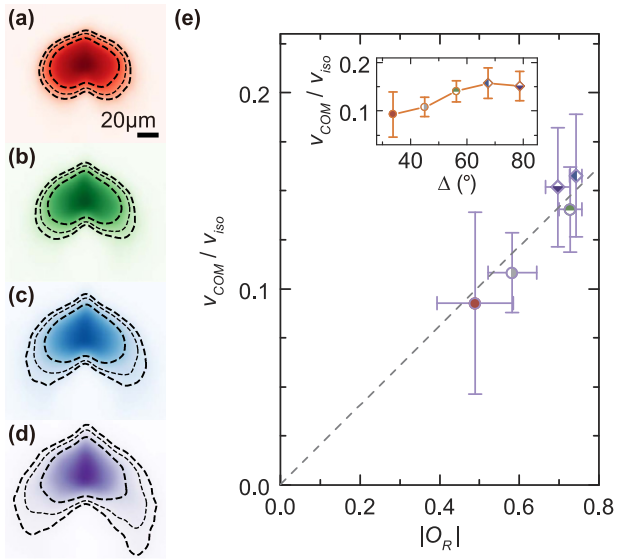

Figure 4. Geometrical shape of an escaping flock as a function of Δ. (a)–(d) AP probability distribution of escaping flocks with $\Delta = [33.75°, 56.25°, 67.5°, 78.75°]$. Dashed lines correspond to the contours where the density has reached [52%, 67%, 75%] of the normalized AP density. (e) Steady state escaping velocity v_{COM} (normalized to the velocity of isolated APs v_{iso}) as a function of $|O_{\mathrm{R}}|$. The error bars correspond to the standard error of the mean obtained from 10 measurements each. Inset: v_{COM} versus deviation angle Δ.

escape velocities. However, given the double vortex structure observed above in the escaping group, this result becomes quite obvious.

3.2. Attentive and inattentive APs

As already mentioned, collective behavior in living systems is believed to provide antipredation benefits. This is obvious since the disadvantage of an increased visibility of dense groups to a predator (compared to that of individuals) must be overcompensated by collective advantages of the group. We also searched for such benefits in our system. Specifically, we considered a scenario where a number of APs are not attentive to a threat (or not informed about its presence) and thus do not respond to it. Hence, the group is divided into initially randomly distributed informed, i.e. threat-sensitive (TS) and uniformed, i.e. threat-inattentive (TI) subgroups which sum up to $N = N_{\mathrm{TS}} + N_{\mathrm{TI}}$.

Figures 5(a) and (b) show the variation of the response delay time τ and escape velocity of groups as a function of N_{TI}/N. The response delay time has been defined as that time after which the group has reached 50% of the steady escape velocity of a group being entirely composed of attentive particles. Remarkably, only when the number of inattentive particles exceeds $\approx 0.5N$, the response delay time τ and the escape velocity significantly deviate compared to $N_{\mathrm{TI}} = 0$. Such outcome demonstrates a clear benefit regarding the group's total attention to threats achieved by cooperative behavior. To understand the origin of this collective advantage, we recall that inattentive APs still respond to attentive ones due to the APs interaction rule (see figures 1(b) and (c)). Obviously, this rule must provide an information flow from attentive to inattentive APs regarding the presence of a threat. To estimate the importance of the two rules governing mutual AP interactions (local particle alignment and collision avoidance), we examined the number of inattentive APs whose left/right swimming decision is decisively determined by attentive particles. We found that this applies to less than $0.1N$. In contrast, attentive particles strongly influence the collision avoidance frequency f_{col} with inattentive particles. When plotting f_{col} as a function of N_{TI}/N we find a maximum at $N_{\mathrm{TI}} \approx 0.6N$ (figure 5(c)) which is near the value where v_{COM} strongly decreases. This suggests that collision avoidance between attentive and inattentive particles provide an important information transfer channel between both particle species. For a qualitative understanding of this effect, it is important to recall that collision avoidance results in particle reorientations. Only when inattentive particles move in parallel with the attentive ones, their orientations receive least disturbance from such collision avoidance events and hence remain rather stable. As collision avoidance only requires short-range interactions, it is hardly disturbed by visual obstruction rendering this mechanism rather robust even within dense populations but also in presence of orientational disorder. Interestingly, the threshold of inattentive particles below which we observe only little changes in the group's response to a threat is only little affected when N is varied between 65 and 165.

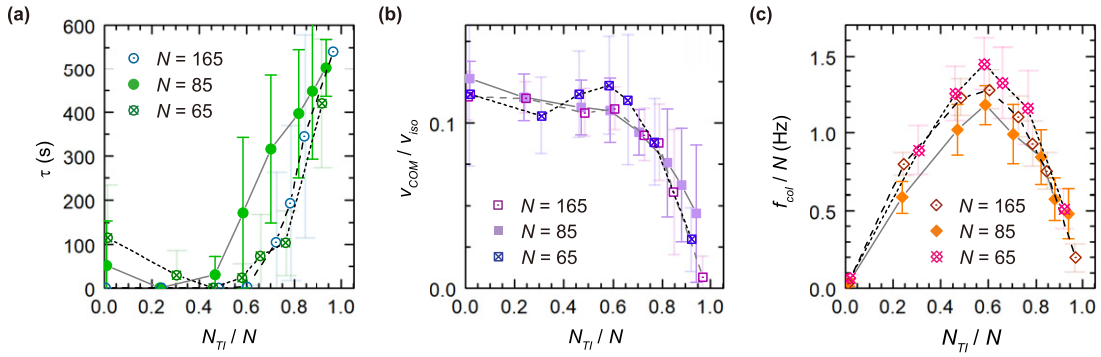

Figure 5. Escape in presence of inattentive particles. (a) Time-delay of the response of the groups to a predator as a function of the fraction of inattentive particles N_{PI}/N. (b) Normalized escape velocity versus N_{PI}/N. (c) Normalized rate of collision-avoidance events between predator attentive and predator inattentive APs as a function of N_{PI}/N. The error bars correspond to the standard error of the mean obtained from 10 measurements each.

4. Discussion

With a system of feedback-controlled active colloidal particles we experimentally study the response and escape of a socially interacting group to an appearing static threat (predator). Since the interaction rules followed by each AP makes only use of the relative position of the hazardous area (threat) and the group's COM, this largely reduces the information to be gathered by each AP regarding the threat leading to robust behavior. Even though, the threat-prey response of a single AP is not necessarily leading to a motion opposite to the prey, in combination with the social interaction with their peers, the overall group's response results in a collective threat avoidance motion. The benefit of such a collective escape behavior is that the group's response to a threat hardly deteriorates even when a considerable fraction of group members does not respond to this threat.

Many other prey–predator social models mimic the response to a predator by a repulsive interaction which typically results in group expansion and splitting. Such behavior can be indeed part of a predator confusion strategy in case of a rapidly approaching predator. Even then, however, there is a general tendency of remerging of the group behind the predator. Such behavior has been also observed in experiments where we considered a predator moving towards the group (opposed to be at rest). Although the passing predator is leading to a large deformation of the group, it immediately reshape after the predator dashed through [see supplementary figure 1 (https://stacks.iop.org/NJP/24/033001/mmedia)].

The flock-like group configuration which generally forms during the group's escape is rather different from what is typically found in Vicsek (or related) models [22, 35]. Opposed to flocking states with only small variance of the polarization within the group, the collective maneuver of our microrobotic group results from the creation of two counter-rotating swirls. Similar mixed collective patterns have been also observed e.g. in schooling fish responding to predators [36].

We want to emphasize, that our experiments are performed in a true physical environment where particle interactions are also influenced by e.g. steric, hydrodynamic and phoretic interactions which are typically omitted in computer simulations. Even though certain aspects, e.g. the group escape motion are well reproduced by simulations (see supplementary figure 2), other aspects such as the hardly affect vigilance below a critical number of inattentive APs is not reproduced in simulations, the latter rather suggesting a continuously decreasing response of the group to a predator as a function of inattentive particles (see supplementary figure 3).

Beyond its relevance for the understanding of collective response of living organisms to a threat, our results have also relevance to micro-robotic systems and show how missing or even false information (e.g. due to sensorial failures or noise) gathered by single robots can be compensated by appropriate interactions within the group. When considering robotic swarms comprised of several thousand interacting agents, such interactions can serve as error correction mechanisms are essential for reliable and failure-resistant performance. While in the case of designing swarms with the behaviors of sub-groups optimized for different tasks or even when implementing hierarchy controls, these interactions work as behavior sharing mechanisms which effectively increase the functionalities of the swarms as a whole.

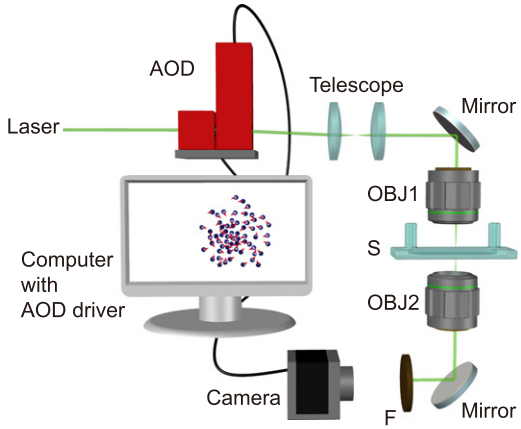

Figure 6. Schematics of the experimental setup and the feedback control cycle. A laser beam is deflected by a pair of acousto-optical deflectors (AOD) for the control of beam position and intensity at the sample, and then guided by a confocal optics to the back aperture of a microscope objective (OBJ1). The focused laser beam then works as the steering signal of the AP suspending inside the sample cell (S). These APs at the lower sample plain are imaged with an appropriate optical system (including OBJ2 and bandpass filter F) onto a camera. The AP configuration is analyzed and used to generate the next steering singles in real-time by a computer.

5. Materials and methods

5.1. Fabrication and properties of active particles

APs are made from colloidal silica spheres with diameter $\sigma = 6.3$ μm which are first prepared as a monolayer. After the solvent has been evaporated, they are coated with a 80 nm carbon cap by thermal evaporation. Afterwards, particles are suspended in a critical water-lutidine mixture and injected into a 200 μm thick sample cell which is kept at $T = 27$ °C, i.e. several degrees below the critical temperature $T_C \approx 34.15$ °C. In presence of light illumination, the particles exhibit active Brownian motion with the propulsion direction opposite to the capped side [32]. Due to gravity and hydrodynamic effects, the APs motion is restricted to two-dimensions [37]. The translational and rotational diffusion constants were experimentally determined to be $D_T = 0.014$ μm^2 s^{-1} and $D_R = 0.0028$ s, respectively.

5.2. Particle motion and individual particle control

Individual AP motion is activated by a local illumination pattern produced by the optical setup shown in figure 6. To form such a pattern, the position and intensity of a focused laser beam with wavelength $\lambda = 532$ nm is controlled by a pair of acousto-optical deflectors (AOD). The deflected beam is then guided into a microscope objective (OBJ1) that focuses the beam at the particle position with the beam waist $w = 5$ μm inside the sample cell (S). Observation of the AP motion is achieved by a second objective (OBJ2) and a camera with a bandpass filter (F) blocking the laser beam. The particle positions and orientations (defined as the vector from the capped side to the uncapped one) are obtained by image analysis on a computer for calculating the laser position.

To impose user-defined interaction rules and to achieve independent AP motion, we take images of the particle configuration at a frequency of 5 Hz. The steering signals determined by the interaction rules are computed with the particle positions and orientations in real time. This information is used to scan a laser beam so each particle is illuminated with a laser spot for 8 μs with a repetition time of 2 ms. Because the remixing timescale of the water-lutidine mixture is about 100 ms, this ensures steady self-propulsion conditions. The (time averaged) intensity of the laser beam is $I_0 = 0.36$ W mm^{-2}, which leads to a propulsion velocity of $v = 0.7$ μm s^{-1}. Controlled reorientation of the APs is achieved by offsetting the laser spot 1.8 μm away from the particle center opposite to the desired direction of motion. This results in a light gradient ∇I across the particle and leads to an inhomogeneous heating of the cap. This causes an asymmetry of the fluid's flow field around the AP relative to its orientation, which eventually leads to a torque and a particle rotation rate $\omega_{max} \approx 4°$ s.

5.3. Determination of the spatially resolved vorticity and alignment within groups

The spatially resolved vorticity is calculated as

$$c(\boldsymbol{r}) = \frac{1}{N}\sum_{i=1}^{N} g\left(\boldsymbol{r}-\boldsymbol{r}_i\right)\frac{\left(\boldsymbol{r}-\boldsymbol{r}_i\right)\times\hat{\boldsymbol{u}}_i^{\mathrm{COM}}}{\left|\boldsymbol{r}-\boldsymbol{r}_i\right|}\hat{\boldsymbol{e}}_z,$$

where N is the total number of particles, $\boldsymbol{r}_i$ a vector pointing to the ith particle and $\hat{\boldsymbol{u}}_i^{\mathrm{COM}}$ its direction of velocity in the reference frame of the COM. To yield a local quantity, contributions are weighted with $g\left(\boldsymbol{r}-\boldsymbol{r}_i\right)$ which is a Gaussian distribution with variance of 2σ.

Acknowledgements

The authors acknowledge stimulating discussions with Francois Lavergne, Robert Löffler and Tobias Bäuerle. This project has received funding from the European Union's Horizon 2020 research and innovation programme under the Marie Skłodowska-Curie Grant Agreement No. 812780, the ERC Advanced Grant ASCIR (No. 693683) and DFG Centre of Excellence 2117 'Centre for the Advances Study of Collective Behaviour', ID: 422037984.

ORCID iDs

Chun-Jen Chen https://orcid.org/0000-0002-4549-8899
Clemens Bechinger https://orcid.org/0000-0002-5496-5268

References

[1] Sumpter D J T 2010 *Collective Animal Behavior* (Princeton, NJ: Princeton University Press)
[2] Krause J and Ruxton G D 2002 *Living in Groups* (Oxford: Oxford University Press)
[3] Penzhorn B L 2010 A long-term study of social organisation and behaviour of Cape mountain zebras equus zebra zebra *Z. Tierpsychologie* **64** 97–146
[4] Parrish J K and Edelstein-Keshet L 1999 Complexity, pattern, and evolutionary trade-offs in animal aggregation *Science* **284** 99–101
[5] Traniello J F A 1989 Foraging strategies of ants *Annu. Rev. Entomol.* **34** 191–210
[6] Rieucau G, De Robertis A, Boswell K M and Handegard N O 2014 School density affects the strength of collective avoidance responses in wild-caught Atlantic herring Clupea harengus: a simulated predator encounter experiment *J. Fish Biol.* **85** 1650–64
[7] Lima S L and Zollner P A 1996 Anti-predatory vigilance and the limits to collective detection: visual and spatial separation between foragers *Behav. Ecol. Sociobiol.* **38** 355–63
[8] Hayward M W and Kerley G I H 2005 Prey preferences of the lion (Panthera leo) *J. Zool.* **267** 309
[9] Waters A, Blanchette F and Kim A D 2012 Modeling huddling penguins *PLoS One* **7** e50277
[10] Feinerman O, Pinkoviezky I, Gelblum A, Fonio E and Gov N S 2018 The physics of cooperative transport in groups of ants *Nat. Phys.* **14** 683–93
[11] Gelblum A, Pinkoviezky I, Fonio E, Gov N S and Feinerman O 2016 Emergent oscillations assist obstacle negotiation during ant cooperative transport *Proc. Natl Acad. Sci. USA* **113** 14615–20
[12] Slavkov I, Carrillo-Zapata D, Carranza N, Diego X, Jansson F, Kaandorp J, Hauert S and Sharpe J 2018 Morphogenesis in robot swarms *Sci. Robot.* **3** eaau9178
[13] Vásárhelyi G, Virágh C, Somorjai G, Nepusz T, Eiben A E and Vicsek T 2018 Optimized flocking of autonomous drones in confined environments *Sci. Robot.* **3** eaat3536
[14] Berlinger F, Gauci M and Nagpal R 2021 Implicit coordination for 3D underwater collective behaviors in a fish-inspired robot swarm *Sci. Robot.* **6** eabd8668
[15] Dorigo M, Theraulaz G and Trianni V 2020 Reflections on the future of swarm robotics *Sci. Robot.* **5** eabe4385
[16] Wang Q and Zhang L 2021 External power-driven microrobotic swarm: from fundamental understanding to imaging-guided delivery *ACS Nano* **15** 149–74
[17] Breder C M 1951 Studies on the structure of the fish school *Bulletin of the AMNH* **98** 1
[18] Ward A J W and Webster M M 2019 Mid-sized groups perform best in a collective decision task in sticklebacks *Biol. Lett.* **15** 20190335
[19] Rieucau G, Holmin A J, Castillo J C, Couzin I D and Handegard N O 2016 School level structural and dynamic adjustments to risk promote information transfer and collective evasion in herring *Animal Behav.* **117** 69–78
[20] Kunz H, Züblin T and Hemelrijk C 2006 On prey grouping and predator confusion in artificial fish schools *10th Int. Conf. Simulation and Synthesis of Living Systems* (Cambridge, MA: MIT Press) pp 365–71
[21] Wood A J and Ackland G J 2007 Evolving the selfish herd: emergence of distinct aggregating strategies in an individual-based model *Proc. R. Soc. B.* **274** 1637–42
[22] Couzin I D, Krause J, James R, Ruxton G D and Franks N R 2002 Collective memory and spatial sorting in animal groups *J. Theor. Biol.* **218** 1–11
[23] Pitcher T J and Wyche C J 1983 Predator-avoidance behaviours of sand-eel schools: why schools seldom split *Predators and Prey in Fishes* (Developments in environmental biology of fishes) (Berlin: Springer) **2** 193–204
[24] Tosh C R, Krause J and Ruxton G D 2009 Basic features, conjunctive searches, and the confusion effect in predator–prey interactions *Behav. Ecol. Sociobiol.* **63** 473–5
[25] Jeschke J M and Tollrian R 2007 Prey swarming: which predators become confused and why? *Animal Behav.* **74** 387–93
[26] Xie H, Sun M, Fan X, Lin Z, Chen W, Wang L, Dong L and He Q 2019 Reconfigurable magnetic microrobot swarm: multimode transformation, locomotion, and manipulation *Sci. Robot.* **4** eaav8006
[27] Sosna M M G, Twomey C R, Bak-Coleman J, Poel W, Daniels B C, Romanczuk P and Couzin I D 2019 Individual and collective encoding of risk in animal groups *Proc. Natl Acad. Sci. USA* **116** 20556–61
[28] Lavergne F A, Wendehenne H, Bäuerle T and Bechinger C 2019 Group formation and cohesion of active particles with visual perception-dependent motility *Science* **364** 70–4

[29] Muiños-Landin S, Fischer A, Holubec V and Cichos F 2021 Reinforcement learning with artificial microswimmers *Sci. Robot.* **6** eabd9285
[30] Chowdhury S, Jing W and Cappelleri D J 2015 Controlling multiple microrobots: recent progress and future challenges *J. Micro-Bio Robot.* **10** 1–11
[31] Wang G *et al* 2021 Emergent field-driven robot swarm states *Phys. Rev. Lett.* **126** 108002
[32] Gomez-Solano J R, Samin S, Lozano C, Ruedas-Batuecas P, van Roij R and Bechinger C 2017 Tuning the motility and directionality of self-propelled colloids *Sci. Rep.* **7** 14891
[33] Tunstrøm K, Katz Y, Ioannou C C, Huepe C, Lutz M J and Couzin I D 2013 Collective states, multistability and transitional behavior in schooling fish *PLoS Comput. Biol.* **9** e1002915
[34] Bäuerle T, Löffler R C and Bechinger C 2020 Formation of stable and responsive collective states in suspensions of active colloids *Nat. Commun.* **11** 2547
[35] Vicsek T, Czirók A, Ben-Jacob E, Cohen I and Shochet O 1995 Novel type of phase transition in a system of self-driven particles *Phys. Rev. Lett.* **75** 1226
[36] Brattstrom B H 1998 Strategies of predator attacks on the schooling fish, selar crumenophthalmus, in Academy Bay, Socorro Island, Islas Revillagigedo *Mexico Bull. Southern Calif. Acad. Sci.* **97** 76–81
[37] Das S, Garg A, Campbell A I, Howse J, Sen A, Velegol D, Golestanian R and Ebbens S J 2015 Boundaries can steer active Janus spheres *Nat. Commun.* **6** 8999